

PAPER

## Strengthening decomposition of oxytetracycline in DBD plasma coupling with Fe-Mn oxide-loaded granular activated carbon


To cite this article: Shoufeng TANG *et al* 2019 *Plasma Sci. Technol.* **21** 025504

View the [article online](#) for updates and enhancements.

### Recent citations

- [Alleviating Na<sup>+</sup> effect on phosphate and potassium recovery from synthetic urine by K-struvite crystallization using different magnesium sources](#)  
Haiming Huang *et al*
- [Defect-engineered cobalt-based solid catalyst for high efficiency oxidation of sulfite](#)  
Jie Liu *et al*
- [Performance of Freshly Generated Magnesium Hydroxide \(FGMH\) for Reactive Dye Removal](#)  
Shiyu Liu *et al*

# Strengthening decomposition of oxytetracycline in DBD plasma coupling with Fe-Mn oxide-loaded granular activated carbon

Shoufeng TANG (唐首锋) , Xue LI (李雪), Chen ZHANG (张晨),  
Yang LIU (刘洋), Weitao ZHANG (张维涛) and Deling YUAN (袁德玲)<sup>1</sup>

Hebei Key Laboratory of Applied Chemistry, School of Environmental and Chemical Engineering,  
Yanshan University, Qinhuangdao 066004, People's Republic of China

E-mail: [yuandeling83@126.com](mailto:yuandeling83@126.com)

Received 20 August 2018, revised 22 October 2018

Accepted for publication 24 October 2018

Published 11 January 2019



CrossMark

## Abstract

A catalytic approach using a synthesized iron and manganese oxide-supported granular activated carbon (Fe-Mn GAC) under a dielectric barrier discharge (DBD) plasma was investigated to enhance the degradation of oxytetracycline (OTC) in water. The prepared Fe-Mn GAC was characterized by x-ray diffraction and scanning electron microscopy, and the results showed that the bimetallic oxides had been successfully spread on the GAC surface. The experimental results showed that the DBD + Fe-Mn GAC exhibited better OTC removal efficiency than the sole DBD and DBD + virgin GAC systems. Increasing the fabricated catalyst and discharge voltage was favorable to the antibiotic elimination and energy yield in the hybrid process. The coupling process could be elucidated by the ozone decomposition after Fe-Mn GAC addition, and highly hydroxyl and superoxide radicals both play significant roles in the decontamination. The main intermediate products were identified by HPLC-MS to study the mechanism in the collaborative system.

Supplementary material for this article is available [online](#)

Keywords: dielectric barrier discharge plasma, Iron and manganese oxides, oxytetracycline decomposition, supported granular activated carbon

(Some figures may appear in colour only in the online journal)

## 1. Introduction

Recently, many studies have reported that more and more antibiotics are being found in the effluent of city sewage treatment plants. This is because antibiotics are designed for defending against bacteria and viruses, and it is hard to remove them by traditional biological and chemical methods [1]. The tetracyclines (TCs) are one of the most widely used antibiotics, and oxytetracycline (OTC) is a significant part of TCs [2]. The residues of OTC not only obstruct the biological

activity of organisms, but they can also disturb the physiological functions of the human body. Therefore, many physical and chemical techniques have been researched for OTC removal, such as adsorption, filtration and some advanced oxidation processes (AOPs) [3–5].

Non thermal plasma (NTP) is a novel AOP which can generate a great amount of reactive species, including ozone ( $O_3$ ), hydrogen peroxide ( $H_2O_2$ ), and hydroxyl radical ( $\cdot OH$ ), as well as various physical impacts such as high-energy electrons, strong field, shockwave, and UV radiation [6, 7]. These effects can decompose organics rapidly and non-selectively [8, 9]. Among the different types of NTPs,

<sup>1</sup> Author to whom any correspondence should be addressed.

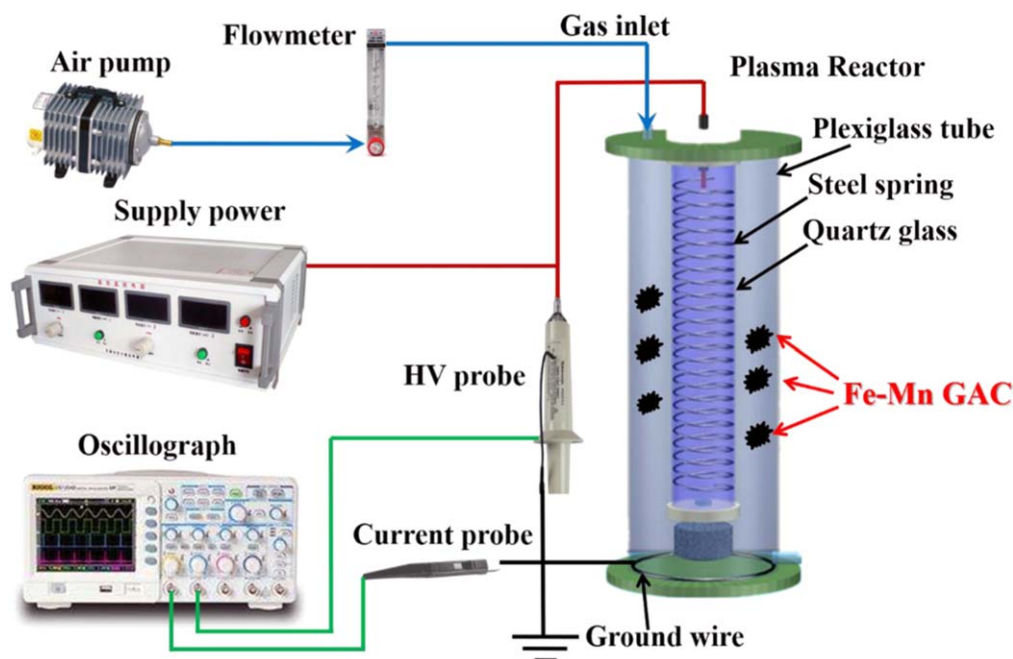


Figure 1. Diagram of the hybrid system.

dielectric barrier discharge (DBD) plasma has been extensively studied since it can be easily and stably generated with a vast array of active substances [10–12]. DBD plasma has been applied to treat environmental contaminants in water, air, and soil [13–15]. However, energy yield is an important limitation to the application of NTP, and an integrated processes with adsorption and catalysis is a potential solution [16, 17]. Herein, pollutants could be preconcentrated on adsorbent, and the multiple strong oxidative species in NTP could be fully utilized by catalytic reactions to form plentiful active species and then remove pollutants thoroughly.

Nowadays, metals and metal oxides are deemed to be effective catalysts in Fenton processes and catalytic ozonation. Among them, the iron and manganese classes are more frequently used due to their high catalysis activity and low price [18–20]. However, there exist numerous defects in the use process, such as low mass transfer and difficulty segregating after the reaction. Hence, these substances should be loaded on a supporter to avoid these deficiencies. Granular activated carbon (GAC) would be well suited to be the carrier, as it has high specific surface area and developed hole structure, prominent adsorbability, and relatively high catalytic activity [21]. Additionally, some research indicates that bimetallic or trimetallic loaded catalysts could improve activity and durability, forming a synergy for the catalytic reaction [22, 23].

Therefore, a Fe-Mn bimetallic oxide supported on GAC (Fe-Mn GAC) has been synthesized and introduced into a DBD system, with the expectation that this will catalytically decompose  $O_3$  and  $H_2O_2$  into more chemically active species such as  $\cdot OH$ , perhydroxyl radicals ( $\cdot HO_2$ ) and superoxide radical ( $\cdot O_2^-$ ), and so on, enhancing the removal of antibiotics and energy efficiency of discharge plasma. The prepared catalyst was characterized by x-ray diffraction (XRD) and

scanning electron microscopy (SEM), and the catalytic performance was determined by investigating the degradation of OTC at different systems, catalyst dosages, and discharge voltages. Moreover, the catalysis mechanism was explored by a quantitative test of dissolved  $O_3$  concentration and examination of diverse radical scavengers. Additionally, the degradation evolution of OTC was proposed based on the analysis of high-performance liquid chromatography–mass spectrometry (HPLC-MS).

## 2. Experimental

### 2.1. Materials and catalyst preparation

A columned coal-based GAC with diameter 2.0 mm and length 1.0–3.0 mm was purchased from Shenyang Chemical Reagent Factory, China. The OTC and other chemical reagents employed in this work were analytical grade reagents. The Fe-Mn GAC was synthesized by an impregnation–desiccation method, and the detailed steps were the same as in our previous study [24].

### 2.2. DBD system

A diagram of the DBD system applied in this study is shown in figure 1. A cylindrical quartz tube with 13 mm inner diameter, 1 mm wall thickness, and 300 mm height was applied as the dielectric. A stainless steel spring with 13 mm outer diameter and 260 mm height clinged to the silica tube inwall as the high-voltage (HV) electrode. An aerator was placed in the bottom of the tube to eject active species into the water. A plexiglass cylinder with 80 mm inner diameter and 430 mm height was used as the wastewater vessel, and then the wastewater was grounded by a wire in the vessel bottom. An air

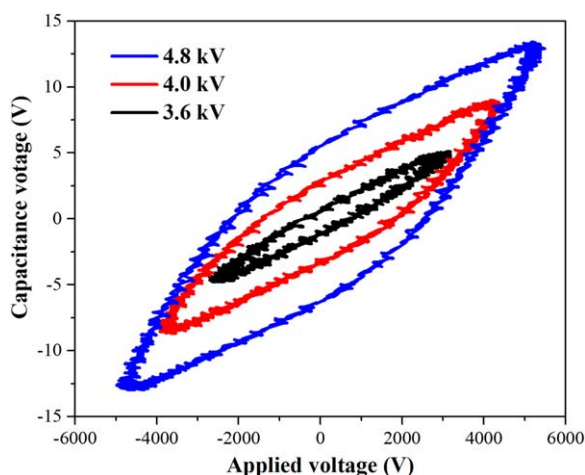


Figure 2. Lissajous diagrams with different discharge voltages.

pump was applied to provide dried gas for discharge, and the flow rate was  $1.0 \text{ L min}^{-1}$ . An AC power source was used to supply power for the reactor, and its frequency was set at 10 kHz.

The Lissajous figures were recorded by an oscilloscope (Rigol, DS2102A) equipped with a voltage probe (Tektronix P6015A) and a low-voltage probe (Rigol, PVP2350), as displayed in figure 2. A  $60 \mu\text{F}$  measuring capacitance was connected with the ground electrode in series. The discharge power was calculated by the following formula:

$$P = f \times C \times S$$

where  $P$  (W) is the reactor power,  $f$  (Hz) is the discharge frequency,  $C$  is the measuring capacitance, and  $S$  is the integral area of the Lissajous figure.

The OTC and its TOC and COD abatement ratio were computed through the following formula:

$$\text{Removal \%} = \frac{C_0 - C}{C_0} \times 100\%$$

where  $C_0$  and  $C$  are the concentrations of the test object at times 0 and  $t$ , respectively.

The energy yield ( $G_{50}$ ,  $\text{mg kJ}^{-1}$ ) for OTC removal was defined as follows:

$$G_{50} = \frac{0.5m_{\text{OTC}}}{P \cdot t_{50}}$$

where  $m_{\text{OTC}}$  (mg) is the amount of decomposed OTC, and  $t_{50}$  (s) is the treatment time when 50% of the OTC was degraded.

### 2.3. Characterization, test, and analysis

XRD (Smart Lab, Rigaku) was used to determine the crystal structure of the GAC samples. SEM (Zeiss SUPRA55) with energy-dispersive x-ray spectroscopy (EDS) was applied to investigate the morphology of the samples.

In each batch experiment, a certain amount of the Fe-Mn GAC and 200 ml prepared OTC solution, with an initial concentration of  $50 \text{ mg L}^{-1}$ , was added into the Plexiglass tube of the reactor before the discharge treatment. The OTC degradation and intermediates were analyzed by a HPLC-MS (Agilent

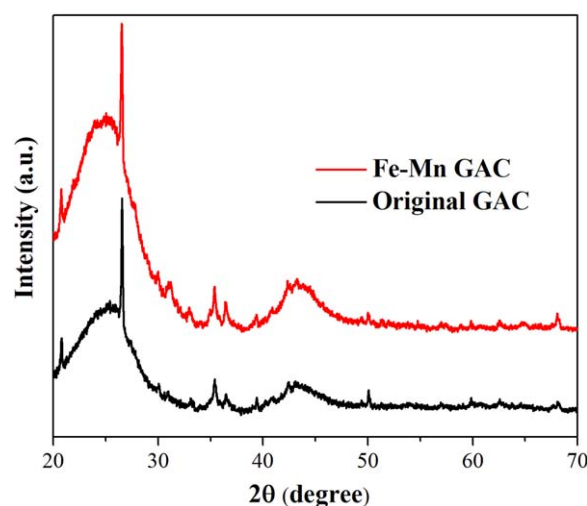


Figure 3. XRD patterns of Fe-Mn GAC and pristine GAC.

6460 Triple Quad LC/MS, USA) using an Agilent Eclipse XDB-C18 analytical reversed-phase column ( $150 \times 4.6 \text{ mm}^2$ ,  $3.5 \mu\text{m}$ ) in positive ion mode. The UV detector of the HPLC was operated at 354 nm, and the mobile phase was comprised of acetic acid and acetonitrile (84:16 v/v) at  $0.2 \text{ ml min}^{-1}$  flow rate. TOC removal was tested by a Shimadzu TOC-V analyzer, and COD removal was measured through the potassium dichromate standard method. The concentration of  $\text{O}_3$  was determined by iodometry method.

## 3. Results and discussion

### 3.1. Characterization of Fe-Mn GAC and GAC

Figure 3 shows the XRD patterns of the Fe-Mn GAC and pristine GAC. The original GAC presented a representative amorphous structure, and the Fe-Mn GAC maintained similar crystal phases after the load of bimetallic oxides. There were no obvious peaks of iron oxide and manganese oxide, which demonstrates that the formative Fe and Mn oxides were also amorphous.

Figure 4 presents the surface morphology and elementary composition before (figures 4(a) and (b)) and after the use of supporting bimetallic metal oxides (figures 4(c) and (d)). Compared with figure 4(a), we can see clearly that some particles were uniformly loaded onto the surface in the bulk of the GAC despite the agglomeration of a few oxides in figure 4(c). Although these formed oxides were deposited on the carbon surface on a large scale, the Fe-Mn GAC still retained the same activated carbon spatial distribution as that in the unmodified state. This feature could provide a favorable space for the adsorption and catalytic reaction among active components, reactive species, and organic molecules, promoting the generation of strong oxidative matters and then enhancing pollutant decontamination directly and indirectly. Moreover, from the EDS data, the element mass ratio of Fe, Mn, and oxygen were all increased in the hybrid material. Among them, the mass percent of Fe and Mn loadings



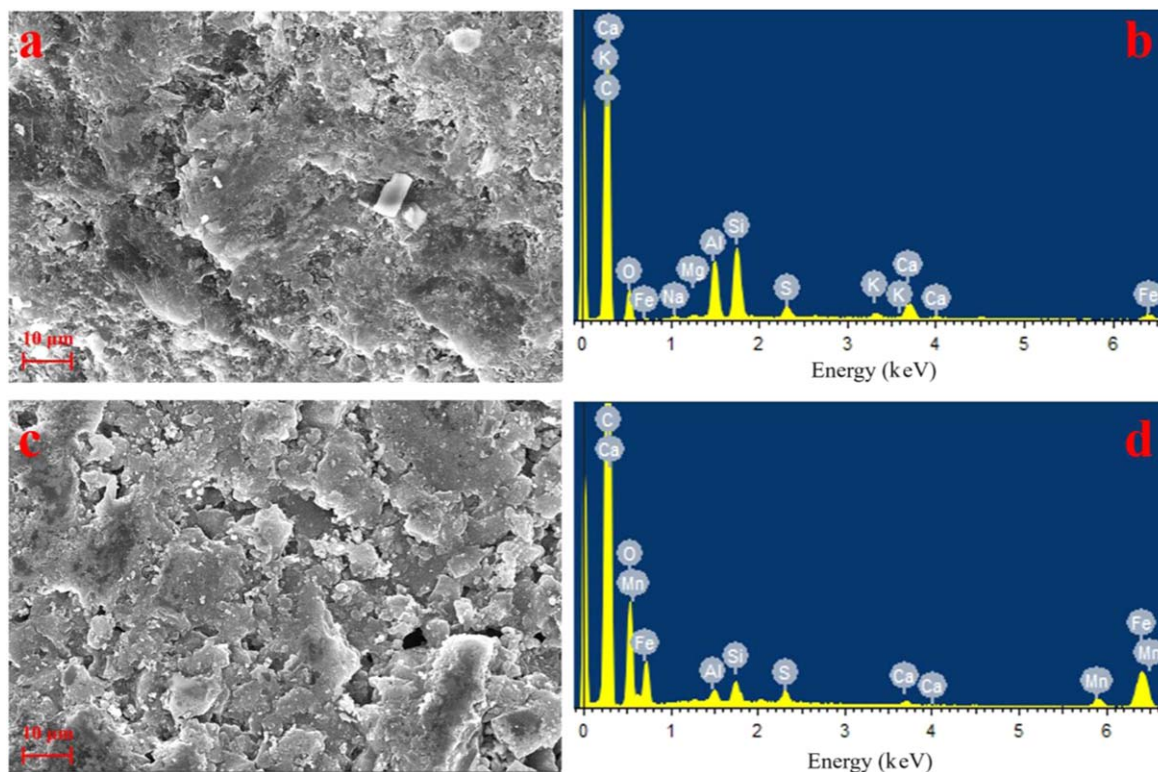


Figure 4. SEM images and EDS spectra of original GAC ((a) and (b)) and Fe-Mn GAC ((c) and (d)).

reached 16.5% and 3.8%, respectively, after the supported process. This result further proves that the Fe and Mn oxides had been successfully immobilized on the surface of coarse GAC after the impregnation–desiccation method.

### 3.2. Enhancement of OTC degradation with Fe-Mn GAC

Figure 5 illustrates the degradation of OTC under different systems. The experimental conditions were the GAC and Fe-Mn GAC of 1 g each, and applied voltage of 4.0 kV. After 20 min, the adsorption capacity of Fe-Mn GAC reached 21.3%, which was marginally reduced by about 2.7% compared with the virgin GAC. This is due to the iron and manganese oxides being supported onto the hole structure of GAC, blocking some of the adoption sites. Besides, it is well known that activated carbon not only plays the role of adsorbent, but is also a good catalyst for ozonation [25, 26]. In this study, O<sub>3</sub> generated from the surface gas-phase DBD configuration was the primary active species in the reactor [27]. It can be seen from this figure that the OTC removal was increased from 82% to 89% after adding GAC to the DBD system. This is because the delocalized π electron on carbon surface triggers a chain reaction of O<sub>3</sub> decomposition to produce more reactive radicals, promoting the OTC elimination [25, 28].

Furthermore, when the bimetallic oxide-loaded GAC was introduced into the DBD system, the OTC degradation efficiency and rate were both improved. The OTC removal was augmented to 93.5% at 20 min. This phenomenon indicated that the hybrid catalyst exhibited better catalytic activity, manifesting in turn that the immobilized component Fe and

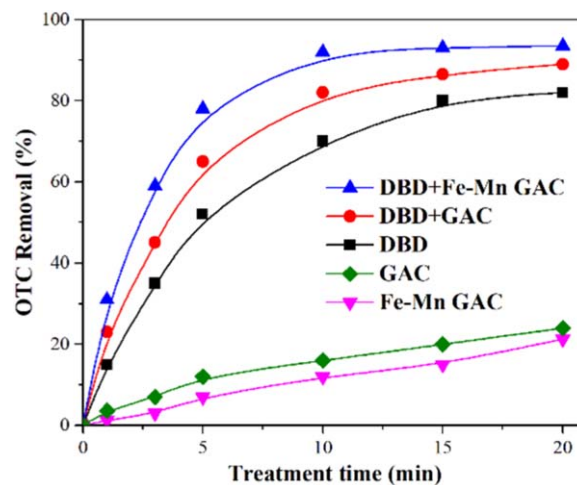
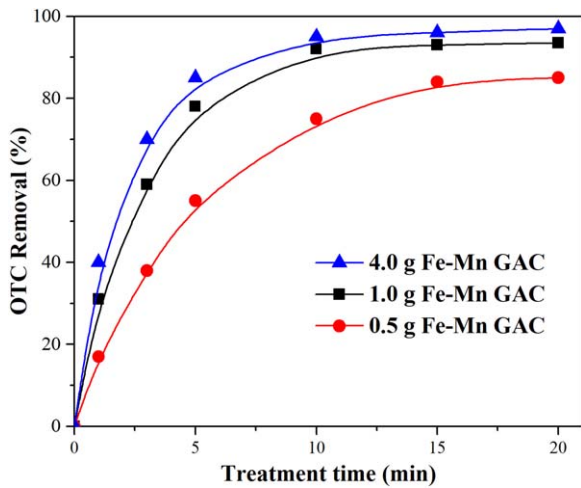


Figure 5. Comparison of OTC degradation under various systems.

Mn oxides could further improve the catalytic effect. It is generally believed that the composite could better catalyze the O<sub>3</sub> decomposition into ·OH, ·HO<sub>2</sub> and ·O<sub>2</sub><sup>-</sup> radicals, further enhancing the decontamination of OTC. Furthermore, the Fe-Mn oxide coating increased the TOC and COD removal ratio, and these experimental results are shown in table 1. After 20 min of treatment, only 36.7% and 21.2% of TOC and COD, respectively, were eliminated in the DBD system, whereas 42.3% and 28.5% of TOC and COD were degraded in the DBD + Fe-Mn GAC system, which were increased by 5.6% and 7.3%, respectively, over the sole DBD treatment. These results corresponded to the above-mentioned OTC degradation tests. Moreover, the calculated G<sub>50</sub> value was

**Table 1.** Comparison of TOC and COD removal under different treatments.

Treatment	TOC removal	COD removal
DBD + Fe-Mn GAC	42.3%	28.5%
DBD	36.7%	21.2%



**Figure 6.** Effect of Fe-Mn GAC dosage on OTC degradation.

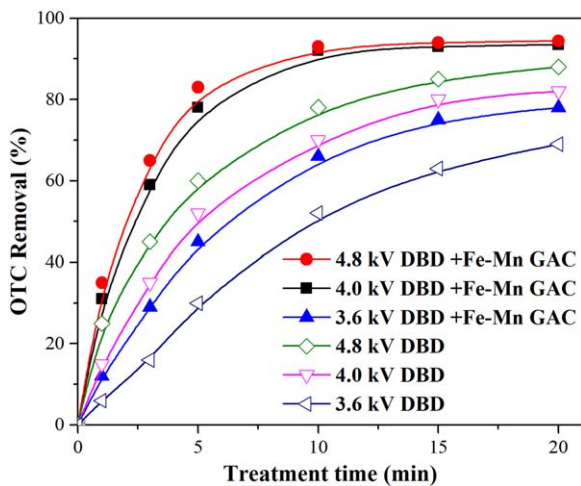


**Figure 7.** Effect of applied voltage on OTC degradation.

0.23 mg kJ<sup>-1</sup> in the DBD + Fe-Mn GAC system, an increase of 33.4% over the single DBD system, suggesting that the introduction of Fe-Mn GAC was also beneficial to the improvement of energy efficiency of discharge plasma.

**3.3. Effect of Fe-Mn GAC dosage on OTC degradation**

Figure 6 shows the effect of Fe-Mn GAC dosage on OTC degradation in the DBD reactor. The applied voltage was 4.0 kV in this section. The results showed that increased hybrid dose was conducive to organics removal. Fe-Mn GAC with 0.5, 1.0, and 4.0 g promoted OTC abatement to 85.2%, 93.5%, and 97.1%, respectively. That is because the addition of more catalyst supplies more active sites of catalysis, benefiting high free radical generation and OTC elimination.

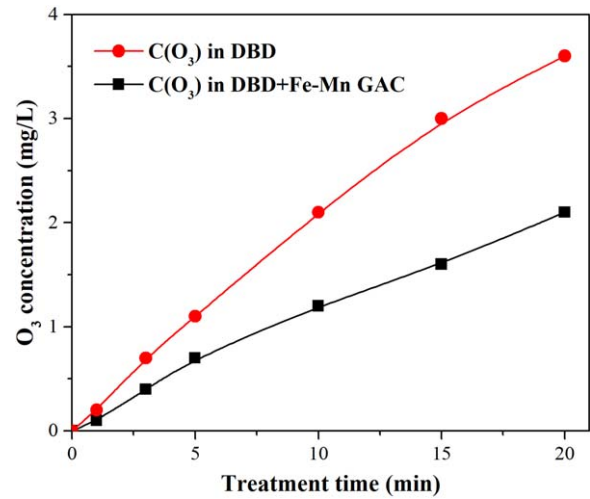


**Figure 8.** O<sub>3</sub> concentrations in the DBD and DBD/Fe-Mn GAC system.

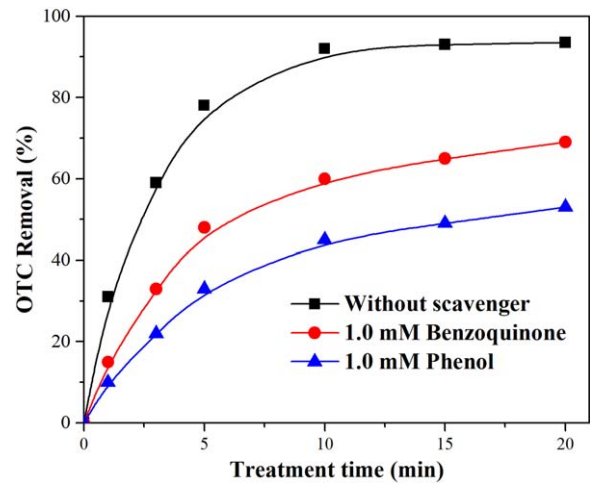


**Figure 9.** Effect of radical scavengers on OTC degradation.

Efficiency was not improved obviously when the catalyst was 4.0 g, so 1.0 g Fe-Mn GAC was selected as the suitable dosage in the subsequent experiments.

**3.4. Effect of applied voltage on OTC degradation**

Figure 7 presents the effect of applied voltage on OTC degradation in the DBD reactor. Obviously, the increasing discharge voltage was favorable to the OTC decomposition in Fe-Mn GAC addition and Fe-Mn GAC free addition. For example, without the catalyst addition, at the 3.6 kV voltage, approximately 69.2% of OTC was removed after 20 min discharge treatment; the removal ratio was enhanced to 82.0% and 88.2% at voltages of 4.0 and 4.8 kV, respectively. Meanwhile, the values of G<sub>50</sub> were 0.11, 0.15, and 0.27 mg kJ<sup>-1</sup> at voltages of 3.6, 4.0, and 4.8 kV, respectively. With the catalyst addition, the degradation efficiencies after 20 min improved to 78.0%, 93.5%, and 94.4% at 3.6, 4.0, and 4.8 kV, respectively. In this case, the G<sub>50</sub> was increased to 0.15, 0.23, and 0.36 mg kJ<sup>-1</sup> at 3.6, 4.0, and 4.8 kV, respectively. It can be concluded that higher voltage would

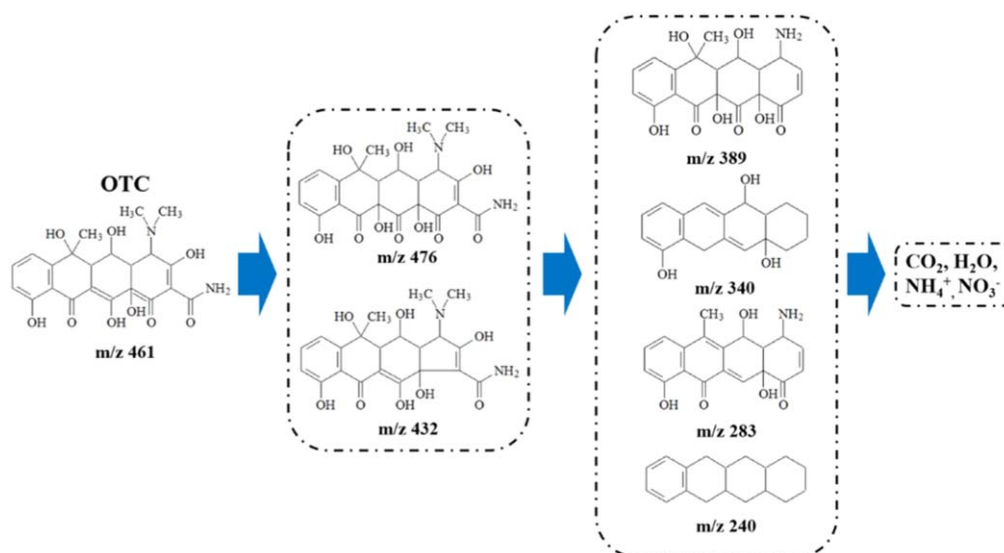


**Figure 10.** Proposed degradation pathway of OTC.

inject greater energy into the reactor and generate more reactive materials, favoring the catalytic reaction generation with synthetic carbon and leading to improvement of the energy utilization and organic compound removal in the DBD system [29, 30].

### 3.5. $O_3$ concentrations in the hybrid system

To further investigate the catalytic process in the DBD + Fe-Mn GAC system, we measured the dissolved  $O_3$  concentration in samples with and without the addition of catalyst; these results are displayed in figure 8. The experimental conditions were applied voltage 4.0 kV and Fe-Mn GAC 1.0 g. It can be noticed that the ozone concentration was reduced after the Fe-Mn GAC addition; the detected  $O_3$  amount was only  $2.1 \text{ mg L}^{-1}$  at 20 min in the synergistic system, a decrease of  $1.5 \text{ mg L}^{-1}$  compared with the sole DBD system. This result shows that a fairly large amount of  $O_3$  might be decomposed to form multiple active species as a previously mentioned reaction mechanism.

### 3.6. Effect of radical scavengers on OTC degradation

In order to reveal the reactive oxidative species in the DBD + Fe-Mn GAC system for OTC degradation, the effects of several typical radical scavengers were analyzed in detail. The experimental conditions were identical with section 3.5.  $\cdot\text{OH}$  and  $\cdot\text{O}_2^-$  radicals were the important final or intermediate products in the catalytic decomposition of  $O_3$ . Phenol can quench  $\cdot\text{OH}$  radicals with the rate constant of  $6.6 \times 10^9 \text{ M}^{-1} \cdot \text{s}^{-1}$ , and benzoquinone is responsible for the  $\cdot\text{O}_2^-$  radical scavenging [31–33]. As depicted in figure 9, excessive phenol (1.0 mM) and benzoquinone (1.0 mM) were added into the coupling system. The results indicated that the OTC degradation efficiency decreased to 53.1% under the presence of phenol, and about 68.8% OTC was removed in the presence of benzoquinone. The obvious suppressions with the

addition of these two scavengers demonstrated that the both  $\cdot\text{OH}$  and  $\cdot\text{O}_2^-$  were produced in the DBD + Fe-Mn GAC system, and these radicals both participate in the OTC degradation process.

### 3.7. Possible OTC degradation mechanism

To assess thoroughly the mechanism of antibiotic decomposition by the hybrid system, HPLC-MS was implemented to analyze the degradation byproducts of OTC in the DBD + Fe-Mn GAC system. Some main decomposition intermediates have been identified, as displayed in figure 10. From the separated peaks of the HPLC/MS chromatograph in the supplementary data (figures S1–S6 are available online at [stacks.iop.org/PST/21/025504/mmedia](https://stacks.iop.org/PST/21/025504/mmedia)), possible intermediates with  $m/z$  of 476, 432, 388, 340, 283, and 239 were speculated. The OTC decomposition mechanism could be attributed to some active species generated from the combined catalytic process of DBD plasma and supported GAC, such as  $\cdot\text{OH}$  and  $\cdot\text{O}_2^-$ . Due to its high redox potential,  $\cdot\text{OH}$  would play a major role in the antibiotic decomposition. Specifically,  $\cdot\text{OH}$  is an electrophilic radical and could attack ethanol and tertiary amine of OTC under hydrogen abstraction reaction because of the increasing electron density of  $\alpha$ -carbon to O in the  $-\text{OH}$  group and N of the  $-\text{NH}_2$  group. Furthermore,  $\cdot\text{OH}$  can also attack the aromatic ring through hydroxy addition reaction on the double bond of the OTC molecule. In addition,  $\cdot\text{OH}$  can trigger an electron transfer reaction to oxidize the organic matrix of OTC. Therefore, combined with the results of HPLC-MS, we concluded that the OTC molecules would be degraded to some intermediate products revealed in figure 10, and then stepwise decomposed to certain smaller molecule compounds and organic acids, and finally to a few inorganic materials [3, 34, 35].

#### 4. Conclusions

We have explored a catalytic way to enhance the degradation of OTC by the addition of Fe-Mn GAC to the DBD reactor. XRD and SEM analysis proved that the hybrid catalyst had been successfully synthesized, and the Fe and Mn oxides were uniformly distributed on the carbon. The catalytic test showed that addition of the bimetallic oxides GAC generated a synergistic effect and improved the OTC degradation efficiency. Increased catalyst dosage and discharge voltage both benefited the antibiotic abatement in the DBD system. Moreover, determinations of O<sub>3</sub> concentration and radical scavengers demonstrated that the catalytic decomposition of O<sub>3</sub> and the function of ·OH and ·O<sub>2</sub><sup>-</sup> radicals were the major synergy mechanisms for organics removal. Lastly, the OTC degradation intermediates were identified by HPLC-MS, and the possible elimination evolution was proposed.

#### Acknowledgments

This work was supported by National Natural Science Foundation of China (No. 51608468), High School Science and Technology Research Project of Hebei Province (No. QN2018258), China Postdoctoral Science Foundation (Nos. 2015M580216 and 2016M601285), and Hebei Province Preferred Postdoctoral Science Foundation (No. B2016003019).

#### ORCID iDs

Shoufeng TANG (唐首锋)  <https://orcid.org/0000-0002-8922-5702>

#### References

- [1] Karaolia P et al 2018 *Appl. Catal. B* **224** 810
- [2] Ren X Y et al 2017 *Chemosphere* **173** 563
- [3] Liu Y Q et al 2016 *Chem. Eng. J.* **284** 1317
- [4] Zhou J X et al 2018 *Colloids Surf. A* **545** 60
- [5] Li N et al 2018 *Electrochim. Acta* **270** 330
- [6] Locke B R and Thagard S M 2012 *Plasma Chem. Plasma Process.* **32** 875
- [7] Jiang N et al 2018 *Chem. Eng. J.* **350** 12
- [8] Wang T C et al 2018 *Environ. Sci. Technol.* **52** 7884
- [9] Jiang B et al 2014 *Chem. Eng. J.* **236** 348
- [10] Xu D et al 2017 *Plasma Sci. Technol.* **19** 064004
- [11] Krupež J et al 2018 *J. Phys. D Appl. Phys.* **51** 174003
- [12] Nayak G et al 2018 *Plasma Process. Polym.* **15** 1700119
- [13] Zhao D et al 2018 *Plasma Sci. Technol.* **20** 014020
- [14] Zhao H et al 2018 *Plasma Sci. Technol.* **20** 035503
- [15] Wang H J et al 2017 *Plasma Sci. Technol.* **19** 015504
- [16] Sun Q N et al 2018 *Environ. Sci. Nano* **5** 2440
- [17] Wang K et al 2018 *Front. Chem. Sci. Eng.* **12** 376
- [18] Chen C M et al 2014 *Fuel Process. Technol.* **124** 165
- [19] Chen C M et al 2014 *J. Ind. Eng. Chem.* **20** 2782
- [20] Wang K et al 2017 *Int. J. Electrochem. Sci.* **12** 8306
- [21] Menya E et al 2018 *Chem. Eng. Res. Des.* **129** 271
- [22] Wolski L and Ziolk M 2018 *Appl. Catal. B* **224** 634
- [23] Ayoub G and Ghauch A 2014 *Chem. Eng. J.* **256** 280
- [24] Tang S F et al 2016 *Environ. Sci. Pollut. Res.* **23** 18800
- [25] Vega E and Valdés H 2018 *Micropor. Mesopor. Mater.* **259** 1
- [26] Luo X N et al 2017 *Nanoscale Res. Lett.* **12** 99
- [27] Cao Y et al 2018 *Plasma Sci. Technol.* **20** 054018
- [28] He X X et al 2017 *J. Hazard. Mater.* **326** 101
- [29] Wang T C et al 2016 *Water Res.* **89** 28
- [30] Duan L J et al 2018 *Plasma Sci. Technol.* **20** 054009
- [31] Du X D et al 2017 *Chem. Eng. J.* **313** 1023
- [32] Wang T C et al 2017 *Environ. Sci. Pollut. Res.* **24** 21591
- [33] Gu J M et al 2018 *Nanoscale* **10** 17722
- [34] Hu X Y et al 2016 *Appl. Surf. Sci.* **362** 329
- [35] Chen Q H, Wu S N and Xin Y J 2016 *Chem. Eng. J.* **302** 377